Proceedings of ASME Turbo Expo 2011
GT2011
June 6-10, 2011, Vancouver, British Columbia, Canada

GT2011-45808

INVERSE PROBLEM FOR ISENTROPIC MACH-NUMBER ON BLADE WALL IN AERODYNAMIC SHAPE DESIGN OF TURBOMACHINERY CASCADES BY USING ADJOINT METHOD

Haitao LI, Liming SONG, Pengfei ZHANG, Zhenping FENG*

Institute of Turbomachinery, School of Energy & Power Engineering
Xi'an Jiaotong University, Xi'an 710049, P. R. China
Phone: +86-29-82665062, Fax: +86-29-82665062
Email: x-lihaitao@hotmail.com, *zpfeng@mail.xjtu.edu.cn

ABSTRACT

This paper presents an approach of the continuous adjoint system deduction based on the variation in grid node coordinates, in which the variation in the gradient of flow quantity is converted into the gradient of the variation in flow quantity and the gradient of the variation in grid node coordinates, which avoids the coordinate system transforming in the traditional derivation process of adjoint system and make the adjoint system much more sententious. By introducing the Jacobian matrix of viscous flux to the gradient of flow variables, the adjoint system for turbomachinery aerodynamic design optimization governed by compressible Navier-Stokes equations is derived in details. Given the general expression of objective functions consisted of both boundary integral and field integral, the adjoint equations and their boundary conditions are derived, and the final expression of the objective function gradient including only boundary integrals is formulated to reduce the CPU cost. Then the adjoint system is numerically solved by using the finite volume method with an explicit 5-step Runge-Kutta scheme and Riemann approximate solution of Roe's scheme combined with multi-grid technique and local time step to accelerate the convergence procedure. Finally, the application of the method is illustrated through a turbine cascade inverse problem with an objective function of isentropic Mach number distribution on the blade wall.

NOMENCLATURE

A, B	Matrices defined in this paper
CFL	Courant-Friedrichs-Lewy number
$\boldsymbol{E}$	State equations
$\boldsymbol{f}_i$	Vector of inviscid flux
$\boldsymbol{f}_{vi}$	Vector of viscous flux
I	Objective function
J	Augmented objective function
M	Field integral term of objective function
Ma	Mach number
N	Boundary integral term of objective function
n_i	Component of outward unit normal vectors
p	Static pressure
p_0	Total pressure at the inlet
$\boldsymbol{Res}$	Vector of numerical residual of adjoint equation
$\boldsymbol{Source}$	Vector of source term of adjoint equation
T	Temperature
u_i	Velocity components
x_i	Cartesian coordinates
α	Design variables
ΔS	Element area
δ	Variation operator with respect to design variables
δ_{ij}	Kronecker symbols
ϕ	Flow quantity
γ	Ratio of specific heats
κ	Thermal conductivity

$\tilde{\Lambda}_c$, $\tilde{T}$	Matrices defined in this paper
Λ_c , Λ_v	Sum of the convective and viscous spectral radii over all faces on the control volume respectively
λ	Second viscosity coefficient
μ	Dynamic viscosity
Π	Variable defined in this paper
ρ	Density
σ_n	Viscous stress of normal direction
τ_{ij} , τ_{in}	Viscous stress
Ω	Volume
$\boldsymbol{\omega}$	Vector of flow variables
$\boldsymbol{\omega}'$	Vector of flow variables gradient with respect to Cartesian coordinates
$\boldsymbol{\psi}$	Vector of adjoint variables

Subscripts and Superscripts

blade	Blade wall boundary
hub	Hub wall boundary
in	Inlet boundary
is	Isentropic
L, *R*	The left and right control volume of the element boundary respectively
n	Normal direction of the surface
out	Outlet boundary
per	Periodical boundary
shroud	Shroud wall boundary
T	Matrix transpose symbol
v	Viscous
wall	Wall boundary
Γ	Boundary of turbomachinery cascade
Ω	Control volume
$\partial\Omega$	Control volume boundary faces

Abbreviation

2D	Two-dimensional
3D	Three-dimensional
CFD	Computational Fluid Dynamics
FMG	Full Multi-grid method
PDEs	Partial differential equations

1. INTRODUCTION

Generally, gradient-based aerodynamic shape optimal design involves a limited number of cost functions (e.g., lift, drag, or target distribution of pressure), but a large number of design variables which are applied to search through a wider range of possible designs and to obtain better performances. Given the large number of design variables, conventional gradient-based methods (e.g. finite differences, complex variables, or linearized approaches) which compute the gradient at a cost proportional to the number of variables are clearly inefficient. On the limit of the current computing resources, the issues focus on aerodynamic shape optimization based on control theory [1-24]. In this method, adjoint system is adopted as the same as optimal control problems, and the gradient of cost functions with respect to design variables can be determined by solving the adjoint equations with coefficients depending on the solution of the flow equations. The cost for solving the adjoint equations is approximate to the cost for solving flow equations, so that sensitivity analysis is independent of the number of design variables and proportional to the number of aerodynamic cost functions. Thus, for aerodynamic shape optimization problems, the adjoint method seems to be an attractive alternative. Two adjoint methods, the continuous and the discrete ones, have been proposed in the literature. In the continuous adjoint method, the adjoint PDEs are first derived from the flow ones and then discretized, and in the discrete one, the discrete adjoint equations are derived directly from the discretized flow equations.

Adjoint method was firstly introduced into fluid dynamics by Pironneau [2], and the first application in aeronautical field was performed by Jameson [3]. Combining the adjoint method with CFD technology, Jameson developed the optimal design method and applied it to a transonic flow case. In succession, Reuther and co-workers published several papers about this approach [4-9], both continuous and discrete methods for inverse problems or direct problems governed respectively by potential equations, Euler equations and Navier-Stokes (N-S) equations. These literatures dealt with problems from the 2D/3D airfoil design to the complex aircraft configurations design, from the drag minimization of wings to the noise reduction of supersonic wings.

In recent years, the adjoint method has been extended into the internal flow in turbomachinery blades for aerodynamic optimization design [10,11]. Now the application of the adjoint method to turbomachinery blading aerodynamic design optimization has become a research focus. Campobasso et al [12] discussed the use of both steady and unsteady discrete adjoint methods for the design of turbomachinery blades. Florea and Hall [13] proposed a discrete adjoint solver based on the time-linearized method for sensitivity analysis of an unsteady inviscid flow through turbomachinery cascades. Wu et al [14], Papadimitriou and Giannakoglou [15,16] developed continuous adjoint solvers for 2D/3D turbomachinery blading aerodynamic design optimization. Li and Feng [17-19] applied the continuous adjoint method to the 2D and 3D inverse design of turbine blades. Wang and He [20,21] successfully employed adjoint aerodynamic design optimization to blades in multi-stage turbomachines. Li and Feng [22] presented an adjoint optimization technique and its application to the design of a transonic turbine cascade by minimizing of entropy generation rate. Luo et al [23] applied a viscous adjoint method to reduce secondary flow loss of a linear cascade by the optimization of blade redesign and endwall contouring. Wang and Li [24] applied the adjoint method to turbomachinery blading aerodynamic design optimization in 3D inverse design and getting rid of flow separation design.

The traditional deduction of the adjoint system method needs to introduce the coordinate transformation matrices [3], and the variation in objective function with respect to design variables should be converted into calculating the variation in objective function with respect to coordinate transformation matrices. Furthermore, when using the continuous adjoint method, how to deal with the viscous term of the flow governing equations and the boundary conditions is still a challenging issue in the adjoint system derivation due to their difficulties. Traditionally, to obtain the viscous term of adjoint equations, the expansion forms of viscous terms in flow governing equations should be given and the variation in viscous stresses should be expressed in terms of variations in the velocity components and geometry [3]. Both above mentioned make the derivation procedure of the adjoint system in viscous flows much more cumbersome and error-prone. Other authors [25] have opted to use the discrete adjoint method combined with automatic differentiation tools to overcome these limitations.

In this paper, an approach of the adjoint system derivation based on the variation in grid node coordinates [16] is applied, in which the variation in the gradient of flow quantity ($\delta(\partial\phi/\partial x_i)$) is converted into the gradient of variation in flow quantity ($\partial(\delta\phi)/\partial x_i$) and the gradient of the variation in grid node coordinates ($\partial(\delta x_k)/\partial x_i$), which avoids the coordinate system transforming in the conventional derivation process of adjoint system and makes the derivation process much more intuitive. By introducing the Jacobian matrix of viscous flow flux to the gradient of flow variables defined in reference [18], the viscous term of adjoint system is derived succinctly and intuitively. For the first time by combining the two methods mentioned above, the adjoint system for the general problem of turbomachinery aerodynamic design optimization governed by compressible Navier-Stokes equations is derived in detail. Given the general expression of objective functions containing both boundary and field contributions, the adjoint equations and their boundary conditions are derived, and the final expression of the objective function gradient with respect to the design variables which depended only on the coordinates' variation along the boundaries of the domain is formulated. Subsequently, the adjoint system is numerically solved by using the finite volume method with an explicit 5-step Runge-Kutta scheme and Riemann approximate solution of Roe's scheme combined with multi-grid technique and local time step to accelerate the convergence procedure. Finally, a numerical example of a turbine cascade inverse problem is presented with an objective function of isentropic Mach number distribution on the blade wall to demonstrate the ability of the present optimization method. Results show that the proposed optimization method has a good performance and can be adapted for the inverse problem in aerodynamic shape design of turbomachinery cascades.

2. ADJOINT FORMULATION OF GENERAL OPTIMIZATION PROBLEM

Aerodynamic shape optimization based on the adjoint method employs the control theory of PDEs system, and the gradient of cost functions with respect to design variables is calculated indirectly by solving the flow governing equations and then the adjoint equations, each only one time, and the repeated calculation for the solution of flow fields has been avoided. As a kind of optimization algorithm based on gradient, the adjoint method makes the computational complexity free of design variable numbers. Being the adjoint method cost independent of the number of design variables, it provides the sensitivity analysis required by gradient-based optimizers in a fast and inexpensive manner.

Here the general aerodynamic shape optimization problem for turbomachinery cascade has been considered. A typical shape optimization problem minimizes an objective function I with respect to the parameterized α of body shape Γ, under the given constrains C_j. The general problem for the aerodynamic optimization of turbine cascades can be described as follows

$$\begin{cases} I(\alpha,\boldsymbol{\omega}) \rightarrow \min\limits_{\alpha\in\Lambda}, \ s.t. \\ \boldsymbol{E}(\alpha,\boldsymbol{\omega}) = 0, \ on\, \Omega_\Gamma \\ C_j(\alpha,\boldsymbol{\omega}) \geq 0, \ 1 \leq j \leq m \end{cases} \tag{1}$$

Where, $\boldsymbol{E}(\alpha,\boldsymbol{\omega}) = 0$ are the N-S equations, which define a unique flow $\boldsymbol{\omega}$ for the given shape Γ in domain Ω_Γ, and constrains $C_j\,(j = 1,2,\cdots,m)$ include geometric and other criteria.

Using Einstein notations, the unsteady N-S equations in Cartesian coordinates can be formulated as

$$\frac{\partial\boldsymbol{\omega}}{\partial t} + \frac{\partial(\boldsymbol{f}_i - \boldsymbol{f}_{vi})}{\partial x_i} = 0, \ i = 1,2\ in\ 2D;\ i = 1,2,3\ in\ 3D \tag{2}$$

in which, the conservation flow variables $\boldsymbol{\omega}$, inviscid flux vector $\boldsymbol{f}_i$, and viscous flux vector $\boldsymbol{f}_{vi}$ are defined in the same way as reference [6].

Introducing the conception of the adjoint system based on the control theory, and defining the adjoint vector as

$$\boldsymbol{\psi} = \{\psi_1,\psi_2,\cdots,\psi_m\}^T, \ m = 4\ in\ 2D;\ m = 5\ in\ 3D \tag{3}$$

in which, the adjoint vector $\boldsymbol{\psi}$ have the same space size of the flow vector $\boldsymbol{\omega}$.

Then, the augmented objective function can be defined as

$$J = I - \int_\Omega \boldsymbol{\psi}^T \left[\frac{\partial\boldsymbol{f}_i - \partial\boldsymbol{f}_{vi}}{\partial x_i}\right] dV \tag{4}$$

which means that the augmented objective function J is identically equal to the objective function I defined in Eq.(1) for the steady flow ($\frac{\partial(\boldsymbol{f}_i - \boldsymbol{f}_{vi})}{\partial x_i} = 0$). To perform the sensitivity analysis, the variation in the augmented objective function J with respect to design variables takes the form

$$\delta J=\delta I-\int_{\Omega}\boldsymbol{\psi}^{T}\delta\left[\frac{\partial(\boldsymbol{f}_i-\boldsymbol{f}_{vi})}{\partial x_i}\right]dV \tag{5}$$

In order to formulate the adjoint problem, Gauss' divergence theorem is applied to reduce the order of flow variable variations, and the variation in the partial derivative in Eq.(5) should be transformed to the partial derivative of a variation. Thus, for any flow quantity ϕ, in reference [16], the formula can be written as

$$\delta\left(\frac{\partial\phi}{\partial x_i}\right)=\frac{\partial(\delta\phi)}{\partial x_i}-\frac{\partial\phi}{\partial x_k}\frac{\partial(\delta x_k)}{\partial x_i} \tag{6}$$

Equation (6) expresses the variation in a spatial derivative of ϕ in terms of the spatial derivative of $\delta\phi$ and the spatial derivative of the variation in position vector (δx_k). Using this equation, the variation in gradients is transformed to gradients of variations avoiding the coordinate system transforming in the conventional derivation process of adjoint system and making the derivation process much more intuitive, and then Gauss' divergence theorem can be employed conveniently.

Subsequently, the adjoint equations and boundary conditions as well as the final formula for the general objective function gradient for viscous flows will be derived. Without loss of generality, the following analysis is valid for 2D or 3D aerodynamic design problems.

2.1 Variation Terms in N-S Equations

The function of the adjoint method is to separate the variations in flow variables and design variables from the variation in the augmented objective function. Thus, Eq.(5) should be expanded. Firstly, and by using Eq.(6) and Gauss' divergence theorem, the second term on the right hand side of Eq.(5) can be written as

$$\begin{aligned}-\int_{\Omega}\boldsymbol{\psi}^{T}\delta\left[\frac{\partial(\boldsymbol{f}_i-\boldsymbol{f}_{vi})}{\partial x_i}\right]dV &=-\oint_{\partial\Omega}\boldsymbol{\psi}^{T}\delta(\boldsymbol{f}_i-\boldsymbol{f}_{vi})n_i dS\\ &+\int_{\Omega}\frac{\partial\boldsymbol{\psi}^{T}}{\partial x_i}\delta(\boldsymbol{f}_i-\boldsymbol{f}_{vi})dV\\ &+\int_{\Omega}\boldsymbol{\psi}^{T}\frac{\partial(\boldsymbol{f}_i-\boldsymbol{f}_{vi})}{\partial x_j}\frac{\partial\delta x_j}{\partial x_i}dV\end{aligned} \tag{7}$$

in which, $\delta(\boldsymbol{f}_i-\boldsymbol{f}_{vi})=\frac{\partial\boldsymbol{f}_i}{\partial\boldsymbol{\omega}}\delta\boldsymbol{\omega}-\frac{\partial\boldsymbol{f}_{vi}}{\partial\boldsymbol{\omega}}\delta\boldsymbol{\omega}-\frac{\partial\boldsymbol{f}_{vi}}{\partial\boldsymbol{\omega}_j'}\delta\boldsymbol{\omega}_j'$, and $\delta\boldsymbol{\omega}_j'=\delta(\frac{\partial\boldsymbol{\omega}}{\partial x_j})=\frac{\partial\delta\boldsymbol{\omega}}{\partial x_j}-\frac{\partial\boldsymbol{\omega}}{\partial x_k}\frac{\partial\delta x_k}{\partial x_j}$, so that the variation in the flow flux can be written as

$$\delta(\boldsymbol{f}_i-\boldsymbol{f}_{vi})=\frac{\partial(\boldsymbol{f}_i-\boldsymbol{f}_{vi})}{\partial\boldsymbol{\omega}}\delta\boldsymbol{\omega}-\frac{\partial\boldsymbol{f}_{vi}}{\partial\boldsymbol{\omega}_j'}(\frac{\partial\delta\boldsymbol{\omega}}{\partial x_j}-\frac{\partial\boldsymbol{\omega}}{\partial x_k}\frac{\partial\delta x_k}{\partial x_j}) \tag{8}$$

In order to avoid transforming the variation in stresses into variations in velocity components and geometry, the Jacobian matrices of inviscid and viscous flux with respect to both the flow variables and gradients of variables should be defined as

$$A_i=\frac{\partial\boldsymbol{f}_i}{\partial\boldsymbol{\omega}},\ A_{vi}=\frac{\partial\boldsymbol{f}_{vi}}{\partial\boldsymbol{\omega}},\ \boldsymbol{\omega}_i'=\frac{\partial\boldsymbol{\omega}}{\partial x_i},\ B=\left[B_{ij}\right]=\left[\frac{\partial\boldsymbol{f}_{vi}}{\partial(\boldsymbol{\omega}_j')}\right] \tag{9}$$

Then Eq.(7) is further rewritten as

$$\begin{aligned}-\int_{\Omega}\boldsymbol{\psi}^{T}\delta\left[\frac{\partial(\boldsymbol{f}_i-\boldsymbol{f}_{vi})}{\partial x_i}\right]dV &=-\oint_{\partial\Omega}\boldsymbol{\psi}^{T}\delta(\boldsymbol{f}_i-\boldsymbol{f}_{vi})n_i dS\\ &+\int_{\Omega}\frac{\partial\boldsymbol{\psi}^{T}}{\partial x_i}\left[(A_i-A_{vi})\delta\boldsymbol{\omega}-B_{ij}\frac{\partial\delta\boldsymbol{\omega}}{\partial x_j}\right]dV\\ &+\int_{\Omega}\frac{\partial\boldsymbol{\psi}^{T}}{\partial x_i}B_{ij}\frac{\partial\boldsymbol{\omega}}{\partial x_k}\frac{\partial\delta x_k}{\partial x_j}dV\\ &+\int_{\Omega}\boldsymbol{\psi}^{T}\frac{\partial(\boldsymbol{f}_i-\boldsymbol{f}_{vi})}{\partial x_j}\frac{\partial\delta x_j}{\partial x_i}dV\end{aligned} \tag{10}$$

In order to disappear the field integrals with respect to the variation of grid node coordinates in the final expression for the augmented objective function gradients, the third and the fourth terms on the right hand side of Eq.(10) should be formulated as follows by using Gauss' divergence theorem,

$$\begin{aligned}\int_{\Omega}\frac{\partial\boldsymbol{\psi}^{T}}{\partial x_i}B_{ij}\frac{\partial\boldsymbol{\omega}}{\partial x_k}\frac{\partial\delta x_k}{\partial x_j}dV &=-\int_{\Omega}\frac{\partial}{\partial x_j}\left(\frac{\partial\boldsymbol{\psi}^{T}}{\partial x_i}B_{ij}\right)\frac{\partial\boldsymbol{\omega}}{\partial x_k}\delta x_k dV\\ &-\int_{\Omega}\frac{\partial\boldsymbol{\psi}^{T}}{\partial x_i}B_{ij}\frac{\partial}{\partial x_j}\left(\frac{\partial\boldsymbol{\omega}}{\partial x_k}\right)\delta x_k dV\\ &+\oint_{\partial\Omega}\frac{\partial\boldsymbol{\psi}^{T}}{\partial x_i}B_{ij}\frac{\partial\boldsymbol{\omega}}{\partial x_k}n_j\delta x_k dS\end{aligned} \tag{11}$$

$$\begin{aligned}\int_{\Omega}\boldsymbol{\psi}^{T}\frac{\partial(\boldsymbol{f}_i-\boldsymbol{f}_{vi})}{\partial x_j}\frac{\partial\delta x_j}{\partial x_i}dV &=-\int_{\Omega}\frac{\partial\boldsymbol{\psi}^{T}}{\partial x_i}\frac{\partial(\boldsymbol{f}_i-\boldsymbol{f}_{vi})}{\partial x_k}\delta x_k dV\\ &-\int_{\Omega}\boldsymbol{\psi}^{T}\frac{\partial}{\partial x_i}\left(\frac{\partial(\boldsymbol{f}_i-\boldsymbol{f}_{vi})}{\partial x_k}\right)\delta x_k dV\\ &+\oint_{\partial\Omega}\boldsymbol{\psi}^{T}\frac{\partial(\boldsymbol{f}_i-\boldsymbol{f}_{vi})}{\partial x_k}n_i\delta x_k dS\end{aligned} \tag{12}$$

In steady N-S equations, there is $\frac{\partial(\boldsymbol{f}_i-\boldsymbol{f}_{vi})}{\partial x_i}=0$, which means that $\frac{\partial}{\partial x_i}\left(\frac{\partial(\boldsymbol{f}_i-\boldsymbol{f}_{vi})}{\partial x_k}\right)=\frac{\partial}{\partial x_k}\left(\frac{\partial(\boldsymbol{f}_i-\boldsymbol{f}_{vi})}{\partial x_i}\right)=0$. And also, there is $\frac{\partial(\boldsymbol{f}_i-\boldsymbol{f}_{vi})}{\partial x_k}=(A_i-A_{vi})\frac{\partial\boldsymbol{\omega}}{\partial x_k}-B_{ij}\frac{\partial}{\partial x_k}\left(\frac{\partial\boldsymbol{\omega}}{\partial x_j}\right)$. So, Eq.(12) can be rewritten as

$$\begin{aligned}&\int_{\Omega}\boldsymbol{\psi}^{T}\frac{\partial(\boldsymbol{f}_i-\boldsymbol{f}_{vi})}{\partial x_j}\frac{\partial\delta x_j}{\partial x_i}dV\\ &=-\int_{\Omega}\frac{\partial\boldsymbol{\psi}^{T}}{\partial x_i}(A_i-A_{vi})\frac{\partial\boldsymbol{\omega}}{\partial x_k}\delta x_k dV\end{aligned}$$

$$+\int_{\Omega}\frac{\partial\boldsymbol{\psi}^T}{\partial x_i}B_{ij}\frac{\partial}{\partial x_k}\left(\frac{\partial\boldsymbol{\omega}}{\partial x_j}\right)\delta x_k dV$$

$$+\oint_{\partial\Omega}\boldsymbol{\psi}^T\frac{\partial(\boldsymbol{f}_i-\boldsymbol{f}_{vi})}{\partial x_k}n_i\delta x_k dS \qquad (13)$$

Therefore, Eq.(11) and Eq.(13) can be summed of

$$\int_{\Omega}\frac{\partial\boldsymbol{\psi}^T}{\partial x_i}B_{ij}\frac{\partial\boldsymbol{\omega}}{\partial x_k}\frac{\partial\delta x_k}{\partial x_j}dV+\int_{\Omega}\boldsymbol{\psi}^T\frac{\partial(\boldsymbol{f}_i-\boldsymbol{f}_{vi})}{\partial x_j}\frac{\partial\delta x_j}{\partial x_i}dV$$

$$=-\int_{\Omega}\left[\frac{\partial\boldsymbol{\psi}^T}{\partial x_i}(A_i-A_{vi})+\frac{\partial}{\partial x_j}\left(\frac{\partial\boldsymbol{\psi}^T}{\partial x_i}B_{ij}\right)\right]\frac{\partial\boldsymbol{\omega}}{\partial x_k}\delta x_k dV$$

$$+\oint_{\partial\Omega}\frac{\partial\boldsymbol{\psi}^T}{\partial x_i}B_{ij}\frac{\partial\boldsymbol{\omega}}{\partial x_k}n_j\delta x_k dS$$

$$+\oint_{\partial\Omega}\boldsymbol{\psi}^T\frac{\partial(\boldsymbol{f}_i-\boldsymbol{f}_{vi})}{\partial x_k}n_i\delta x_k dS \qquad (14)$$

Using Gauss' divergence theorem in the second term on the right hand side of Eq.(10) and combining Eq.(14), the final expression of the variation in N-S equations can be written as

$$-\int_{\Omega}\boldsymbol{\psi}^T\delta\left[\frac{\partial(\boldsymbol{f}_i-\boldsymbol{f}_{vi})}{\partial x_i}\right]dV$$

$$=\int_{\Omega}\left[\frac{\partial\boldsymbol{\psi}^T}{\partial x_i}(A_i-A_{vi})+\frac{\partial}{\partial x_j}(\frac{\partial\boldsymbol{\psi}^T}{\partial x_i}B_{ij})\right]\left(\delta\boldsymbol{\omega}-\frac{\partial\boldsymbol{\omega}}{\partial x_k}\delta x_k\right)dV$$

$$+\oint_{\partial\Omega}\frac{\partial\boldsymbol{\psi}^T}{\partial x_i}B_{ij}\frac{\partial\boldsymbol{\omega}}{\partial x_k}n_j\delta x_k dS+\oint_{\partial\Omega}\boldsymbol{\psi}^T\frac{\partial(\boldsymbol{f}_i-\boldsymbol{f}_{vi})}{\partial x_k}n_i\delta x_k dS$$

$$-\oint_{\partial\Omega}\frac{\partial\boldsymbol{\psi}^T}{\partial x_i}B_{ij}\delta\boldsymbol{\omega}n_j dS-\oint_{\partial\Omega}\boldsymbol{\psi}^T\delta(\boldsymbol{f}_i-\boldsymbol{f}_{vi})n_i dS \qquad (15)$$

With the help of previous expressions, the variation in N-S equations is transformed into field integral and boundary integrals. In order to take into account the boundary conditions (inlet, outlet, wall and periodical boundary) of N-S equations, the boundary integrals of Eq.(15) will be discussed in detail as follows.

Inlet and outlet boundary integral terms

In N-S equations, the flow viscous effect on the inlet and outlet boundary can be neglected. And the boundary integral of Eq.(15) at the inlet and outlet can be written as

$$\int_{in,out}\boldsymbol{\psi}^T\delta(\boldsymbol{f}_i)n_i dS=\int_{in,out}\boldsymbol{\psi}^T A_i n_i\delta\boldsymbol{\omega}dS \qquad (16)$$

where, $i=1,2$ in 2D and $i=1,2,3$ in 3D.

Solid wall boundary integral term

Due to the non-slip boundary condition of the N-S equations on the solid wall ($u_i=0$), the solid wall boundary integral term of Eq.(15) can be formulated as

$$-\int_{wall}\boldsymbol{\psi}^T\delta(\boldsymbol{f}_i-\boldsymbol{f}_{vi})n_i dS-\int_{wall}\frac{\partial\boldsymbol{\psi}^T}{\partial x_i}B_{ij}\delta\boldsymbol{\omega}n_j dS$$

$$=-\int_{wall}\left[\psi_{i+1}p-\boldsymbol{\psi}^T\left(\boldsymbol{f}_i-\boldsymbol{f}_{vi}\right)\right]\delta n_i dS-\int_{wall}\kappa\frac{\partial\psi_m}{\partial n}\delta T dS$$

$$-\int_{wall}\left[\psi_{i+1}\left(n_i\delta p-\delta\tau_{in}\right)-\kappa\psi_m\delta\left(\frac{\partial T}{\partial n}\right)\right]dS \qquad (17)$$

where, $i=1,2;\ m=4$ in 2D and $i=1,2,3;\ m=5$ in 3D.

Periodical boundary integral term

The curvilinear integrals are counteracted on periodical boundary, i.e.

$$\int_{per}\frac{\partial\boldsymbol{\psi}^T}{\partial x_i}B_{ij}\delta\boldsymbol{\omega}n_j dS=\int_{per}\boldsymbol{\psi}^T\delta(\boldsymbol{f}_i-\boldsymbol{f}_{vi})n_i dS=0 \qquad (18)$$

Finally, upon substitution of Eq.(16), Eq.(17) and Eq.(18) into Eq.(15), the variation in N-S equations can be formulated as

$$-\int_{\Omega}\boldsymbol{\psi}^T\delta\left[\frac{\partial(\boldsymbol{f}_i-\boldsymbol{f}_{vi})}{\partial x_i}\right]dV$$

$$=\int_{\Omega}\left[\frac{\partial\boldsymbol{\psi}^T}{\partial x_i}(A_i-A_{vi})+\frac{\partial}{\partial x_j}(\frac{\partial\boldsymbol{\psi}^T}{\partial x_i}B_{ij})\right]\left(\delta\boldsymbol{\omega}-\frac{\partial\boldsymbol{\omega}}{\partial x_k}\delta x_k\right)dV$$

$$+\oint_{\partial\Omega}\frac{\partial\boldsymbol{\psi}^T}{\partial x_i}B_{ij}\frac{\partial\boldsymbol{\omega}}{\partial x_k}n_j\delta x_k dS+\oint_{\partial\Omega}\boldsymbol{\psi}^T\frac{\partial(\boldsymbol{f}_i-\boldsymbol{f}_{vi})}{\partial x_k}n_i\delta x_k dS$$

$$-\int_{in,out}\boldsymbol{\psi}^T A_i n_i\delta\boldsymbol{\omega}dS-\int_{in,out}\frac{\partial\boldsymbol{\psi}^T}{\partial x_i}B_{ij}\delta\boldsymbol{\omega}n_j dS$$

$$-\int_{wall}\left[\psi_{i+1}\left(n_i\delta p-\delta\tau_{in}\right)-\kappa\frac{\partial\psi_m}{\partial n}\delta T+\kappa\psi_m\delta\left(\frac{\partial T}{\partial n}\right)\right]dS$$

$$-\int_{wall}\left[\psi_{i+1}p-\boldsymbol{\psi}^T(\boldsymbol{f}_i-\boldsymbol{f}_{vi})\right]\delta n_i dS \qquad (19)$$

2.2 Variation Terms in Objective Function

For the general aerodynamic design of turbomachinery cascade, the objective function can be formulated as

$$I(\alpha,\boldsymbol{\omega})=\int_{\Omega}M\left(\boldsymbol{\omega}(\alpha),\boldsymbol{\omega}'(\alpha)\right)dV+\int_{\Gamma}N\left(\boldsymbol{\omega}(\alpha)\right)dS \qquad (20)$$

This is feasible in design problems where the objective function is either a boundary integral (e.g. pressure deviation along the solid walls) or a field integral (e.g. the entropy generation over the flow domain). And its variation can be formulated as

$$\delta I=\int_{\Omega}\delta(M)dV+\int_{\Omega}M\delta(dV)+\int_{\Gamma}\delta(N)dS+\int_{\Gamma}N\delta(dS) \qquad (21)$$

As the same as Eq.(10), the field integrals with respect to the variation of grid node coordinates in the final expression for the augmented objective function gradients should be disappeared, and the first and the second term of Eq.(21) should be formulated by using Gauss' divergence theorem.

$$\int_{\Omega}\delta(M)dV=\int_{\Omega}\left(\frac{\partial M}{\partial\boldsymbol{\omega}}\delta\boldsymbol{\omega}+\frac{\partial M}{\partial\boldsymbol{\omega}_i'}\partial\boldsymbol{\omega}_i'\right)dV$$

$$=\int_{\Omega}\frac{\partial M}{\partial\boldsymbol{\omega}}\delta\boldsymbol{\omega}dV+\int_{\Omega}\frac{\partial M}{\partial\boldsymbol{\omega}_i'}\frac{\partial}{\partial x_i}\left(\frac{\partial\boldsymbol{\omega}}{\partial x_k}\right)\delta x_k dV$$

$$-\int_{\Omega}\frac{\partial}{\partial x_i}\left(\frac{\partial M}{\partial\boldsymbol{\omega}_i'}\right)\left(\delta\boldsymbol{\omega}-\frac{\partial\boldsymbol{\omega}}{\partial x_k}\delta x_k\right)dV$$

$$+\oint_{\partial\Omega}\frac{\partial M}{\partial\boldsymbol{\omega}_i^{'}}n_i\delta\boldsymbol{\omega}dS-\oint_{\partial\Omega}\frac{\partial M}{\partial\boldsymbol{\omega}_i^{'}}\frac{\partial\boldsymbol{\omega}}{\partial x_k}n_i\delta x_k dS \tag{22}$$

According to reference [16], the variation of the finite volume $\delta\left(dV\right)$ is expressed in terms of dV

$$\delta\left(dV\right)=\frac{\partial(\delta x_k)}{\partial x_k}dV \tag{23}$$

Therefore, the second term of Eq.(21) can be expanded as

$$\begin{aligned}
&\int_\Omega M\,\delta(dV)=\int_\Omega M\,\frac{\partial(\delta x_k)}{\partial x_k}dV\\
&=-\int_\Omega\frac{\partial M}{\partial x_k}\delta x_k dV+\oint_{\partial\Omega}Mn_k\delta x_k dS\\
&=-\int_\Omega\left(\frac{\partial M}{\partial\boldsymbol{\omega}}\frac{\partial\boldsymbol{\omega}}{\partial x_k}+\frac{\partial M}{\partial\boldsymbol{\omega}_i^{'}}\frac{\partial\boldsymbol{\omega}_i^{'}}{\partial x_k}\right)\delta x_k dV+\oint_{\partial\Omega}Mn_k\delta x_k dS\\
&=-\int_\Omega\frac{\partial M}{\partial\boldsymbol{\omega}}\frac{\partial\boldsymbol{\omega}}{\partial x_k}\delta x_k dV-\int_\Omega\frac{\partial M}{\partial\boldsymbol{\omega}_i^{'}}\frac{\partial}{\partial x_k}\left(\frac{\partial\boldsymbol{\omega}}{\partial x_i}\right)\delta x_k dV\\
&\quad+\oint_{\partial\Omega}Mn_k\delta x_k dS
\end{aligned} \tag{24}$$

From Eq.(21), Eq.(22) and Eq.(24), the objective function variation finally reads

$$\begin{aligned}
\delta I&=\int_\Omega\delta(M)dV+\int_\Omega M\,\delta(dV)+\int_\Gamma\delta(N)dS+\int_\Gamma N\delta(dS)\\
&=\int_\Omega\left[\frac{\partial M}{\partial\boldsymbol{\omega}}-\frac{\partial}{\partial x_i}\left(\frac{\partial M}{\partial\boldsymbol{\omega}_i^{'}}\right)\right]\left(\delta\boldsymbol{\omega}-\frac{\partial\boldsymbol{\omega}}{\partial x_k}\delta x_k\right)dV\\
&\quad-\oint_{\partial\Omega}\frac{\partial M}{\partial\boldsymbol{\omega}_i^{'}}\frac{\partial\boldsymbol{\omega}}{\partial x_k}n_i\delta x_k dV+\oint_{\partial\Omega}Mn_k\delta x_k dV\\
&\quad+\oint_{\partial\Omega}\frac{\partial M}{\partial\boldsymbol{\omega}_i^{'}}\delta\boldsymbol{\omega}n_i dS\\
&\quad+\int_\Gamma\delta_{\boldsymbol{\omega}}\left(N\right)dS+\int_\Gamma\delta_\alpha\left(N\right)dS+\int_\Gamma N\delta\left(dS\right)
\end{aligned} \tag{25}$$

2.3 Variation in Augmented Objective Function

Upon substitution of Eq.(19) and Eq. (25) into Eq.(5), the variation in the augmented objective function can be finally expressed as

$$\begin{aligned}
&\delta J=\delta I-\int_\Omega\boldsymbol{\psi}^T\delta\left[\frac{\partial(\boldsymbol{f}_i-\boldsymbol{f}_{vi})}{\partial x_i}\right]dV\\
&=\underbrace{\int_\Omega\left[\frac{\partial\boldsymbol{\psi}^T}{\partial x_i}(A_i-A_{vi})+\frac{\partial}{\partial x_j}(\frac{\partial\boldsymbol{\psi}^T}{\partial x_i}B_{ij})+\frac{\partial M}{\partial\boldsymbol{\omega}}-\frac{\partial}{\partial x_i}(\frac{\partial M}{\partial\boldsymbol{\omega}_i^{'}})\right]\left(\delta\boldsymbol{\omega}-\frac{\partial\boldsymbol{\omega}}{\partial x_k}\delta x_k\right)dV}_{AdjEQ}\\
&\underbrace{+\oint_{\partial\Omega}\frac{\partial M}{\partial\boldsymbol{\omega}_i^{'}}\delta\boldsymbol{\omega}n_i dS-\int_{in,out}\boldsymbol{\psi}^T A_i n_i\delta\boldsymbol{\omega}dS+\int_\Gamma\delta_{\boldsymbol{\omega}}\left(N\right)dS}_{AdjBC}\\
&\underbrace{-\int_{wall}\left[\psi_{i+1}\left(n_i\delta p-\delta\tau_{in}\right)-\kappa\psi_m\delta\left(\frac{\partial T}{\partial n}\right)+\kappa\frac{\partial\psi_m}{\partial n}\delta T\right]dS}_{AdjBC}\\
&\underbrace{-\int_{wall}\left[\psi_{i+1}p-\boldsymbol{\psi}^T(\boldsymbol{f}_i-\boldsymbol{f}_{vi})\right]\delta n_i dS+\int_\Gamma\delta_\alpha\left(N\right)dS+\int_\Gamma N\delta\left(dS\right)}_{Grad}\\
&\underbrace{-\oint_{\partial\Omega}\frac{\partial M}{\partial\boldsymbol{\omega}_i^{'}}\frac{\partial\boldsymbol{\omega}}{\partial x_k}n_i\delta x_k dS+\oint_{\partial\Omega}\boldsymbol{\psi}^T\frac{\partial(\boldsymbol{f}_i-\boldsymbol{f}_{vi})}{\partial x_k}n_i\delta x_k dS}_{Grad}\\
&\underbrace{+\oint_{\partial\Omega}\frac{\partial\boldsymbol{\psi}^T}{\partial x_i}B_{ij}\frac{\partial\boldsymbol{\omega}}{\partial x_k}n_j\delta x_k dS+\oint_{\partial\Omega}Mn_k\delta x_k dS}_{Grad}
\end{aligned} \tag{26}$$

As shown in Eq.(26), it consists of three parts, the variation terms in flow variables over the flow domain (marked with *AdjEQ*); the variation terms in flow variables along the boundary (marked with *AdjBC*); and the variation terms in grid-coordinate (marked with *Grad*). Therefore, the adjoint system for aerodynamic shape design of turbomachinery cascade can be naturally derived in the following section.

2.4 Adjoint System for General Problem

The adjoint system consists of the adjoint equations, the boundary condition of adjoint equations and the objective function derivatives. From Eq.(26), the adjoint equation of the adjoint system can be described by choosing $\boldsymbol{\psi}$ to ensure the field integral marked with *AdjEQ* to be zero,

$$\frac{\partial\boldsymbol{\psi}^T}{\partial x_i}(A_i-A_{vi})+\frac{\partial}{\partial x_j}(\frac{\partial\boldsymbol{\psi}^T}{\partial x_i}B_{ij})+\frac{\partial M}{\partial\boldsymbol{\omega}}-\frac{\partial}{\partial x_i}(\frac{\partial M}{\partial\boldsymbol{\omega}_i^{'}})=0 \tag{27}$$

with boundary conditions of adjoint system determined by

$$\begin{aligned}
&-\int_{wall}\left[\psi_{i+1}\left(n_i\delta p-\delta\tau_{in}\right)-\kappa\psi_m\delta\left(\frac{\partial T}{\partial n}\right)+\kappa\frac{\partial\psi_m}{\partial n}\delta T\right]dS\\
&+\oint_{\partial\Omega}\frac{\partial M}{\partial\boldsymbol{\omega}_i^{'}}\delta\boldsymbol{\omega}n_i dS+\int_\Gamma\delta_{\boldsymbol{\omega}}\left(N\right)dS\\
&-\int_{in,out}\boldsymbol{\psi}^T A_i n_i\delta\boldsymbol{\omega}dS=0
\end{aligned} \tag{28}$$

It should be indicated that the coefficients of δp, $\delta\tau_{in}$, δT must be zero to ensure Eq.(28), which means that under the given adiabatic wall condition boundary the operator N needs to contain surface pressure, viscous stress and temperature. Considering that the coefficient of δT is linear independent of that of δp, $\delta\tau_{in}$ and can be zero, therefore N must contain surface pressure and viscous stress.

Finally, the remaining terms in Eq.(26), denoted by *Grad*, can be expressed as the augmented objective function derivatives with respect to the design variables

$$\begin{aligned}
\delta J=&\oint_{\partial\Omega}\frac{\partial\boldsymbol{\psi}^T}{\partial x_i}B_{ij}\frac{\partial\boldsymbol{\omega}}{\partial x_k}n_j\delta x_k dS+\oint_{\partial\Omega}Mn_k\delta x_k dS\\
&-\oint_{\partial\Omega}\frac{\partial M}{\partial\boldsymbol{\omega}_i^{'}}\frac{\partial\boldsymbol{\omega}}{\partial x_k}n_i\delta x_k dS+\oint_{\partial\Omega}\boldsymbol{\psi}^T\frac{\partial(\boldsymbol{f}_i-\boldsymbol{f}_{vi})}{\partial x_k}n_i\delta x_k dS\\
&-\int_{wall}\left[\psi_{i+1}p-\boldsymbol{\psi}^T(\boldsymbol{f}_i-\boldsymbol{f}_{vi})\right]\delta n_i dS\\
&+\int_\Gamma\delta_\alpha\left(N\right)dS+\int_\Gamma N\delta\left(dS\right)
\end{aligned} \tag{29}$$

As shown in the equation above, although the function to be minimized is a field integral over the whole computational domain, the final expression for the augmented objective function gradient includes only boundary integrals which can readily be calculated, and it simplifies the calculations to reduce the CPU cost by avoiding computing the variation of each internal grid node coordinate with respect to the design variables, especially for the complex 3D configurations.

3. NUMERICAL TECHNIQUE FOR SOLVING ADJOINT EQUATION

Just as the unsteady N-S equations are solved to find the asymptotic solution to the steady equation, the adjoint equations, Eq.(27) are augmented to an unsteady hyperbolic system of euqations to be numerically solved via marching in the time-direction. Based on the numerical technique of the N-S equations, the augmented unsteady equations for adjoints can be formed as

$$\frac{\partial \boldsymbol{\psi}}{\partial t} - (A_i^T - A_{vi}^T)\frac{\partial \boldsymbol{\psi}}{\partial x_i} - \frac{\partial}{\partial x_j}(B_{ij}^T \frac{\partial \boldsymbol{\psi}}{\partial x_i}) - \frac{\partial M}{\partial \boldsymbol{\omega}} + \frac{\partial}{\partial x_i}(\frac{\partial M}{\partial \boldsymbol{\omega}_i'}) = 0 \quad (30)$$

Using the finite volume method in the N-S equations, the integral form of the adjoint equations in the control volume Ω can be expressed as

$$\int_\Omega \frac{\partial \boldsymbol{\psi}}{\partial t} dV - \oint_{\partial\Omega} (A_i^T - A_{vi}^T) n_i \boldsymbol{\psi} dS - \oint_{\partial\Omega} B_{ij}^T n_j \frac{\partial \boldsymbol{\psi}}{\partial x_i} dS$$
$$- \int_\Omega \left[\frac{\partial M}{\partial \boldsymbol{\omega}} - \frac{\partial}{\partial x_i}(\frac{\partial M}{\partial \boldsymbol{\omega}_i'}) \right] dV = 0 \quad (31)$$

Hence the semi-discretized form of the adjoint equations is

$$\frac{1}{\Omega}\frac{\partial \boldsymbol{\psi}}{\partial t} - \sum_{\partial\Omega} \underbrace{\left[(A_n^T - A_{vn}^T)\boldsymbol{\psi}\Delta S \right]}_{FluxA} - \sum_{\partial\Omega} \underbrace{\left(B_{in}^T \frac{\partial \boldsymbol{\psi}}{\partial x_i} \Delta S \right)}_{FluxB}$$
$$- \boldsymbol{Source}(\boldsymbol{\psi}) = 0 \quad (32)$$

where, $A_n = A_i n_i$, $A_{vn} = A_{vi} n_i$, $B_{in} = B_{ij} n_j$, and the source term is defined as $\boldsymbol{Source}(\boldsymbol{\psi}) = \int_\Omega \left[\frac{\partial M}{\partial \boldsymbol{\omega}} - \frac{\partial}{\partial x_i}(\frac{\partial M}{\partial \boldsymbol{\omega}_i'}) \right] dV$.

In Eq.(32), Roe's approximate Riemann scheme is implemented to calculate the convective fluxes (marked with *FluxA*) of the adjoint equations, while a second-order central difference scheme is adopted to discretize the third derivative items (marked with *FluxB*). Hence,

$$FluxA\big|_{\partial\Omega} = \frac{\Delta S}{2}\{ (A_n - A_{vn})^T\big|_L \boldsymbol{\psi}_L + (A_n - A_{vn})^T\big|_R \boldsymbol{\psi}_R$$
$$+ \left|A_{Roe}\right|^T (\boldsymbol{\psi}_R - \boldsymbol{\psi}_L) \} \quad (33)$$

$$FluxB\big|_{\partial\Omega} = \frac{\Delta S}{4}\left(B_{in}^T\big|_L + B_{in}^T\big|_R \right)\left(\frac{\partial \boldsymbol{\psi}}{\partial x_i}\bigg|_L + \frac{\partial \boldsymbol{\psi}}{\partial x_i}\bigg|_R \right) \quad (34)$$

and the residual vector of the adjoint equations is defined as

$$\boldsymbol{Res}(\boldsymbol{\psi}) = \sum_{\partial\Omega} \frac{\Delta S}{2}\{ (A_n - A_{vn})^T\big|_L \boldsymbol{\psi}_L + (A_n - A_{vn})^T\big|_R \boldsymbol{\psi}_R$$
$$+ \left|A_{Roe}\right|^T (\boldsymbol{\psi}_R - \boldsymbol{\psi}_L) \}$$
$$+ \sum_{\partial\Omega} \frac{\Delta S}{4}\left(B_{in}^T\big|_L + B_{in}^T\big|_R \right)\left(\frac{\partial \boldsymbol{\psi}}{\partial x_i}\bigg|_L + \frac{\partial \boldsymbol{\psi}}{\partial x_i}\bigg|_R \right) \quad (35)$$

in which, L and R denote the left and right control volume of the element boundary $\partial\Omega$, respectively, and $\left|A_{Roe}\right|$ denotes the so-called Roe matrix. As the same as the definition of $A_{Roe} = \tilde{T}\tilde{\Lambda}_c\tilde{T}^{-1}$ in the N-S equations, $\tilde{T}^{-1}$ denotes the matrix of left eigenvectors, $\tilde{T}$ of right eigenvectors and $\tilde{\Lambda}_c$ represents the diagonal matrix of eigenvalues, and they are evaluated by using Roe's averaging [26]. Then, Eq.(32) can be evaluated as

$$\frac{1}{\Omega}\frac{\partial \boldsymbol{\psi}}{\partial t} = \boldsymbol{Res}(\boldsymbol{\psi}) + \boldsymbol{Source}(\boldsymbol{\psi}) \quad (36)$$

In the present paper, an explicit 5-step Runge-Kutta scheme is applied for the time term in the equation above,

$$\boldsymbol{\psi}^0 = \boldsymbol{\psi}^n \quad (37)$$

$$\boldsymbol{\psi}^i = \boldsymbol{\psi}^{i-1} + \alpha_i \frac{\Delta t|_\Omega}{\Omega}\left[\boldsymbol{Res}(\boldsymbol{\psi}^{i-1}) + \boldsymbol{Source}(\boldsymbol{\psi}^{i-1}) \right] \quad (38)$$

$$\boldsymbol{\psi}^{n+1} = \boldsymbol{\psi}^5 \quad (39)$$

In which, $i = 1 \sim 5$, $\alpha_1 = \frac{1}{4}$, $\alpha_2 = \frac{1}{6}$, $\alpha_3 = \frac{3}{8}$, $\alpha_4 = \frac{1}{2}$, $\alpha_5 = 1$, $\frac{\Delta t|_\Omega}{\Omega} = \frac{\mathrm{CFL}}{\Lambda_c + C \cdot \Lambda_v}$. $\Delta t|_\Omega$ denotes the local time step to accelerate the convergence procedure and CFL denotes the Courant-Friedrichs-Lewy number, Λ_c and Λ_v represent a sum of the convective and viscous spectral radii over all faces on the control volume, which are defined in the same way as reference [26], and $C = 4$ is usually used.

To accelerate convergence, a Full Multi-grid (FMG) method in reference [26] is implemented. In this method, the restriction operator is defined as a sum of the residuals from all cells which are contained in one coarse-grid control volume, and the prolongation of the coarse-grid correction is defined as a zeroth-order prolongation operator.

4. INVERSE DESIGN OF TURBINE BLADE

In this section, a numerical example of a turbine cascade inverse problem is presented with an objective function of isentropic Mach number distribution on the blade wall to demonstrate the ability of the present optimization method. Here, the objective function is defined as follows

$$I = \frac{1}{2}\int_{blade} \left(Ma_{is} - Ma_{is}^d \right)^2 dS \quad (40)$$

where, $Ma_{is} = \sqrt{\frac{2}{\gamma-1}\left[\left(\frac{p_0}{p}\right)^{\frac{\gamma-1}{\gamma}} - 1\right]}$, p_0 is the total pressure on the inlet, p is the static pressure on the blade wall, and Ma_{is}^d is the prescribed isentropic Mach number distribution. It means that there are $M(\alpha,\boldsymbol{\omega},\boldsymbol{\omega}') = 0$, $\Gamma = blade$ and $N(\alpha,\boldsymbol{\omega}) = \frac{1}{2}\left(Ma_{is} - Ma_{is}^d\right)^2$ in Eq.(20). The variation in objective function is

$$\delta I = \int_{blade} \Pi \delta p dS + \frac{1}{2}\int_{blade}\left(Ma_{is} - Ma_{is}^d\right)^2 \delta\left(dS\right) \quad (41)$$

in which $\Pi = \frac{1}{\gamma p_0 Ma_{is}}\left(\frac{p}{p_0}\right)^{\frac{1-2\gamma}{\gamma}}\left(Ma_{is} - Ma_{is}^d\right)$.

Just as the previous description, for boundary inverse problem, the operator N must contain surface pressure and viscous stresses. But in viscous flows, the relation $\frac{\partial u_n}{\partial n} = 0$ over the solid wall nodes leads to $\sigma_n = 0$ (see Appendix A), and Eq.(41) can be switched as

$$\delta I = \int_{blade} \Pi\left(\delta p - \delta\sigma_n\right) dS + \frac{1}{2}\int_{blade}\left(Ma_{is} - Ma_{is}^d\right)^2 \delta\left(dS\right) \quad (42)$$

due to $\sigma_n = n_i \tau_{in}$, $n_i n_i = 1$, the variation in the objective function can be formulated as

$$\delta I = \int_{blade}\left[\Pi n_i\left(n_i \delta p - \delta\tau_{in}\right) - \Pi\tau_{in}\delta n_i\right] dS + \frac{1}{2}\int_{blade}\left(Ma_{is} - Ma_{is}^d\right)^2 \delta\left(dS\right) \quad (43)$$

Upon substitution of Eq.(43) into Eq.(27), Eq.(28) and Eq.(29), the adjoint system for the present inverse problem can be formulated subsequently.

Adjoint equation of present inverse design

In the present inverse problem, it only considers the flow quantity distribution on blade wall and the objective function $M(\alpha,\boldsymbol{\omega},\boldsymbol{\omega}')$ equals to zero. Thus, the adjoint equation is written as

$$\frac{\partial \boldsymbol{\psi}^T}{\partial x_i}(A_i - A_{vi}) + \frac{\partial}{\partial x_j}\left(\frac{\partial \boldsymbol{\psi}^T}{\partial x_i} B_{ij}\right) = 0 \quad (44)$$

Blade wall boundary condition

Here, the adiabatic wall boundary condition of the N-S equations is imposed on the blade surface, and it can be written as $\frac{\partial T}{\partial n} = 0$, and also $\delta\left(\frac{\partial T}{\partial n}\right) = 0$. Finally, the blade wall boundary condition of adjoint equation can be formulated as

$$\begin{cases} \psi_{i+1} = \Pi n_i \\ \frac{\partial \psi_m}{\partial n} = 0 \end{cases} \quad (45)$$

where, $i = 1,2; m = 4$ in 2D and $i = 1,2,3; m = 5$ in 3D.

Similarly, if boundary condition of the N-S equations is given with surface temperature and can be written as $T = constant$ and $\delta T = 0$, then the blade wall boundary condition can be expressed as

$$\begin{cases} \psi_{i+1} = \Pi n_i \\ \psi_m = 0 \end{cases} \quad (46)$$

Inlet and outlet boundary conditions

On the inlet and outlet sides, the curvilinear integral should be equal to zero and viscous effects can be neglected, the inlet and outlet boundary conditions are

$$\int_{in,out} \boldsymbol{\psi}^T A_i n_i \delta\boldsymbol{\omega} dS = 0 \quad (47)$$

For the inlet and outlet boundary conditions, by using Thompson's time-related boundary condition theory for hyperbolic PDEs, the detailed discussion is the same as that of the adjoint equation presented by reference [17].

Hub and shroud wall boundary conditions

In the case of 3D, the hub and shroud wall boundary conditions can be derived as

$$\begin{cases} \psi_2 = \psi_3 = \psi_4 = 0 \\ \frac{\partial \psi_5}{\partial n} = 0 \ \textit{for adiabatic wall}; \textit{or } \psi_5 = 0 \ \textit{for isothermal wall} \end{cases} \quad (48)$$

Sensitivity analysis

In this paper, the blade shape is parameterized by using B-splines and the design variables (denoted as α) consist of control dots coordinates of B-splines. Using a differential method, the derivative of cost function can be estimated by making a small perturbation on design variables. Due to the fixed computation domain in the body-fitted coordinates, the grid node coordinates have fixed values at the cascade inlet and outlet; and the periodic boundary integral is offset, the gradient of augmented objective function with respect to the design variables is finally written as follows in two cases.

1) In case of 2D

$$\begin{aligned} \frac{dJ}{d\alpha} = & \int_{blade} \frac{\partial \boldsymbol{\psi}^T}{\partial x_i} B_{ij} \frac{\partial \boldsymbol{\omega}}{\partial x_k} n_j \frac{\delta x_k}{\delta \alpha} dS \\ & + \int_{blade} \boldsymbol{\psi}^T \frac{\partial(\boldsymbol{f}_i - \boldsymbol{f}_{vi})}{\partial x_k} n_i \frac{\delta x_k}{\delta\alpha} dS \\ & - \int_{blade}\left[\psi_{i+1} p - \boldsymbol{\psi}^T(\boldsymbol{f}_i - \boldsymbol{f}_{vi})\right]\frac{\delta n_i}{\delta\alpha} dS \\ & - \int_{blade} \Pi \tau_{in} \frac{\delta n_i}{\delta\alpha} dS \\ & + \frac{1}{2}\int_{blade}\left(Ma_{is} - Ma_{is}^d\right)^2 \frac{\delta(dS)}{\delta\alpha} \end{aligned} \quad (49)$$

2) In case of 3D

$$\frac{dJ}{d\alpha}=\int_{hub,shroud,blade}\frac{\partial\boldsymbol{\psi}^T}{\partial x_i}B_{ij}\frac{\partial\boldsymbol{\omega}}{\partial x_k}n_j\frac{\delta x_k}{\delta\alpha}dS$$
$$+\int_{hub,shroud,blade}\boldsymbol{\psi}^T\frac{\partial(\boldsymbol{f}_i-\boldsymbol{f}_{vi})}{\partial x_k}n_i\frac{\delta x_k}{\delta\alpha}dS$$
$$-\int_{hub,shroud,blade}\left[\psi_{i+1}p-\boldsymbol{\psi}^T(\boldsymbol{f}_i-\boldsymbol{f}_{vi})\right]\frac{\delta n_i}{\delta\alpha}dS$$
$$-\int_{blade}\Pi\tau_{in}\frac{\delta n_i}{\delta\alpha}dS$$
$$+\frac{1}{2}\int_{blade}\left(Ma_{is}-Ma_{is}^d\right)^2\frac{\delta(dS)}{\delta\alpha}\qquad(50)$$

After the gradient is obtained, a gradient-based steepest descent method is applied to the optimization.

Numerical example and discussion

In this paper, the adjoint system of the inverse problem described previously is applied to a 2D turbine cascade by modifying its isentropic Mach number distribution. Table 1 shows the working condition of the test cascade.

Tab. 1 Working conditions of the cascade

Working medium	Air
Total inlet temperature (K)	1,600.0
Total inlet pressure (Pa)	2,489,000.0
Inlet axial flow angle (deg)	0.0
Static outlet pressure (Pa)	1,140,000.0
Wall properties	Adiabatic smooth surface
Blade numbers	36
Pitch diameter (m)	0.282

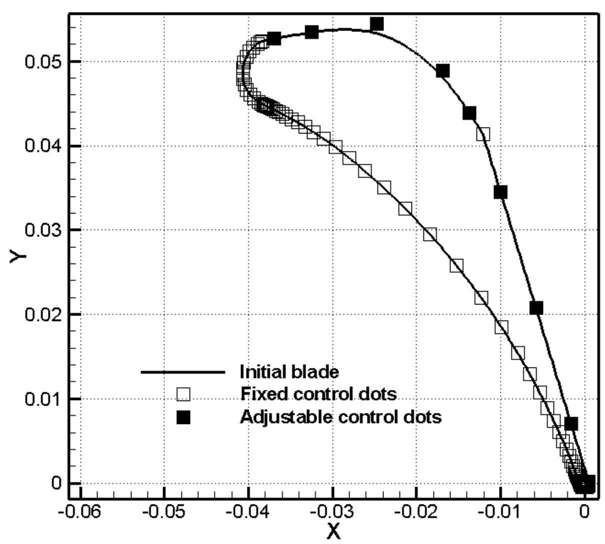

Fig. 1 Designed blade and control dots

The numerical simulations of flow fields are performed by solving the steady compressible Laminar N-S equation using ANSYS CFX 11.0. The boundary conditions are listed in Table 1. The total temperature (1,600.0 K), the total pressure (2,489,000.0 Pa), and the axial flow angle (0^o) are given at the inlet. The outlet static pressure is 1,140,000.0 Pa. The desired convergent target of each simulations is that the root mean square residuals of the momentum and mass equations, energy equation reach (or even lower than) 10^{-6}. The gradient of the objective function is calculated using the continuous adjoint formulation described previously. The 2D blade shape consists of suction and pressure surfaces parameterized by using B-splines.

In the present inverse problem of isentropic Mach number distribution, the source codes of the optimization system are programmed by C++, and the codes include several modules, such as blade profile parameterization by B-splines, automatic mesh generation, ANSYS CFX 11.0 integrated by text-based input files, adjoint PDEs solved by time-marching finite volume method, sensitivity calculation with mesh perturbation and steepest descent algorithm.

The original blade and its B-splines control points are shown in Fig. 1. During the design process, only the suction side of original blade is changed and 8 control points of the B-splines are selected as design control dots. The leading edge, throat point and trailing edge of suction profile are fixed in order to satisfy the restriction on blade geometry.

In this numerical computation, two-grid scheme is taken and the CFL number is selected as 3. Convergence history of the adjoint solvers for the initial cascade is shown in Fig. 2; and the residual of the adjoint equations reaches 10^{-12} in 5000 iterative steps of coarse grid and 10000 iterative steps of fine grid.

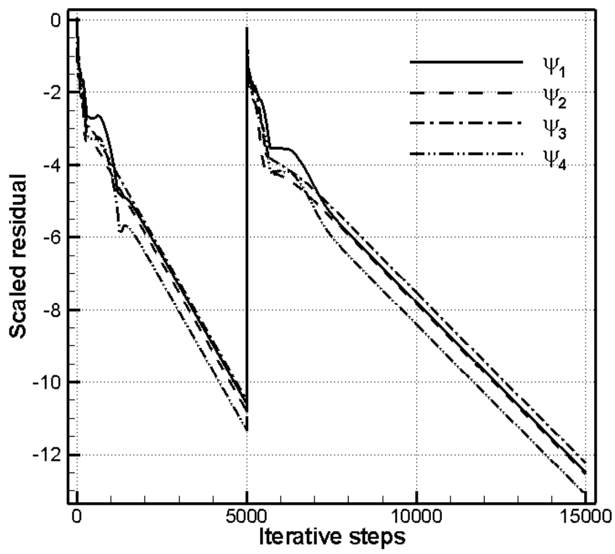

Fig. 2 Convergence history of adjoint solver

The adjoint fields of the initial cascade are given in Fig. 3. It is shown that the largest partial gradient occurs at the throat section of the cascade (which can also be seen in Fig. 8, the 4th and 5th adjustable control dots).

Figures 4, 5 and 6 give the comparisons of blade profile, suction side curvature distribution and isentropic Mach number distribution respectively. They show that the design result agrees well with the aim isentropic Mach number, and the optimal blade profile is much smoother (especially at the throat section, see in Fig. 5).

With 8 design variables the optimization gets convergence by 76 iterative steps and takes 148 times flow

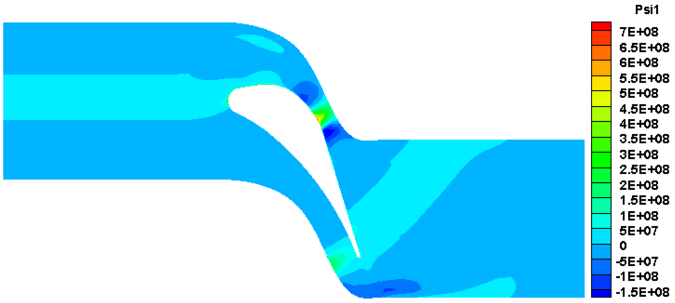

a) Distribution of ψ_1

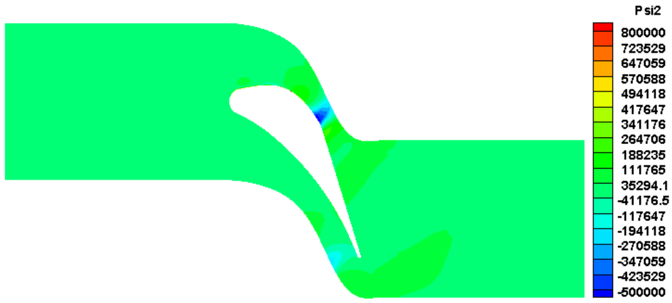

b) Distribution of ψ_2

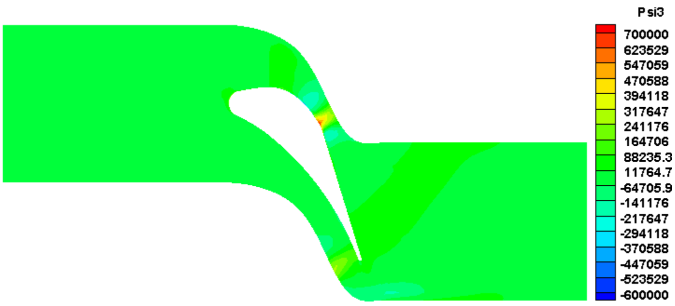

c) Distribution of ψ_3

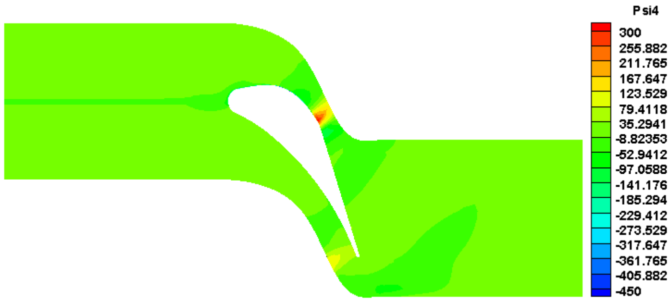

d) Distribution of ψ_4

Fig. 3 Adjoint fields contours of the initial cascade

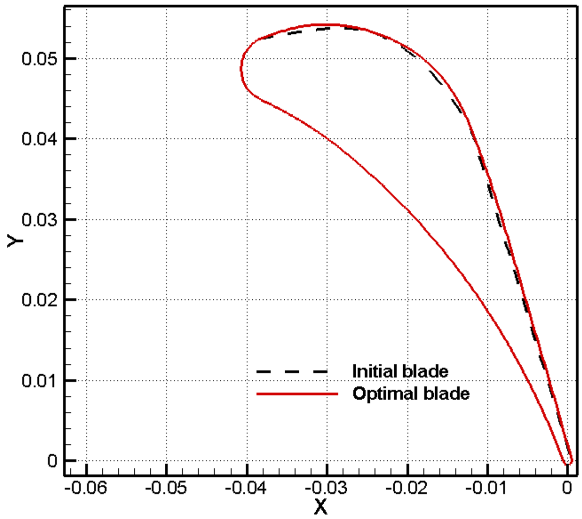

Fig. 4 Blade geometry comparisons

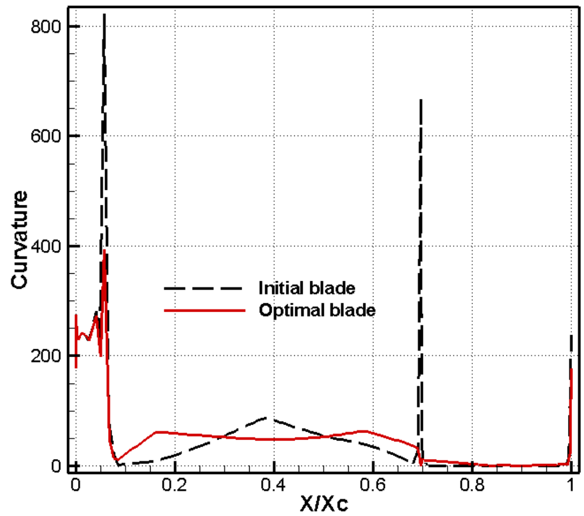

Fig. 5 Suction side curvature distribution

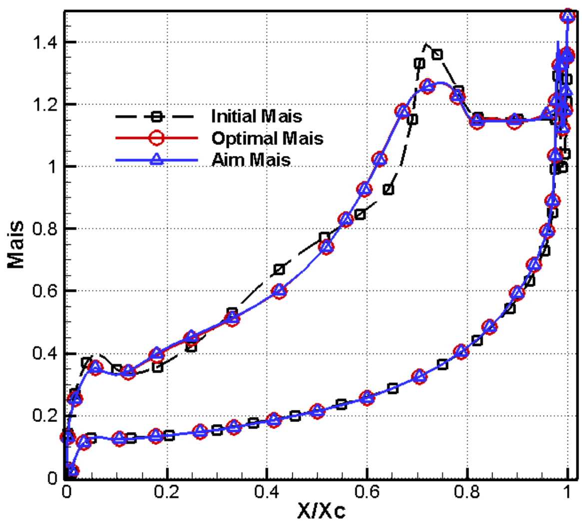

Fig. 6 Isentropic-Mach number distribution

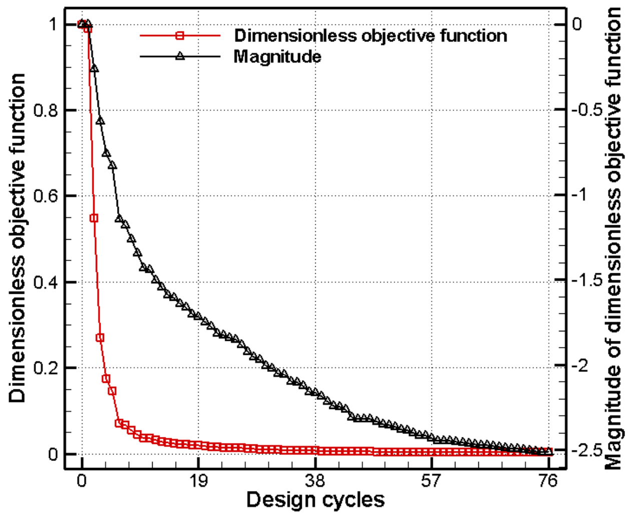

Fig. 7 Scaled convergence history of objective function

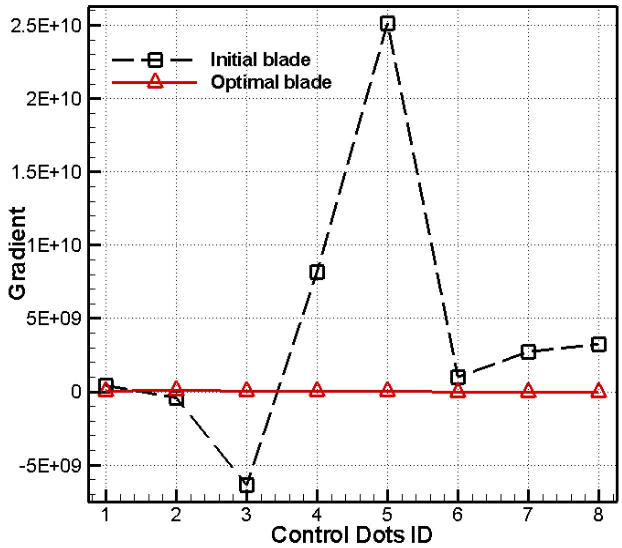

Fig. 8 Gradient components comparisons

filed computation, the residual of objective function reaches $10^{-2.5}$. The scaled convergence history of objective function is shown in Fig. 7, and the contrast diagram of the objective function gradient with respect to design variables between initial and optimal blades is shown in Fig. 8. It indicates that the gradient magnitude of optimal blade is reduced significantly in comparison to initial blade, and the gradient of optimal blade is nearly zero. The reverse design process falls into a local optimal solution, and the optimization gets the comparative optimal blade in an acceptable time.

5. CONCLUSIONS

In the present work, an aerodynamic inverse design method for turbine cascade in viscous flows is developed by using the continuous adjoint method and N-S equations. The important features of the proposed formulation are as follows: firstly, the adjoint system is deducted based on the variation in grid node coordinates and the Jacobian matrices of inviscid and viscous fluxes; secondly, the computation of the objective function gradient is exclusively based on boundary integrals, and the repetitive grid generation of the cascade passage could be avoided in order to reduce the CPU cost, especially in complex 3D configurations; and finally, the adjoint system is numerically solved by using the finite volume method with an explicit 5-step Runge-Kutta scheme and Riemann approximate solution of Roe's scheme combined with multi-grid technique and local time step to accelerate the convergence procedure.

The present method is validated by a turbine cascade inverse problem with an objective function of isentropic Mach number distribution on the blade wall. For boundary inverse problem, in order to figure out blade wall boundary condition of viscous adjoint system, the variation in objective function is redefined by introducing the variation in normal direction viscous stress which should be zero. Results show that the design result agrees well with the aimed isentropic Mach number, and the gradient magnitude of the optimal blade is reduced significantly in comparison with that of the initial blade. The reverse design process falls into a local optimal solution, and the optimization gets the comparative optimal blade in an acceptable time. The numerical results demonstrate that the adjoint equation solver in this paper can work effectively, and the present turbomachinery aerodynamic design optimization is available and has advantages both in accuracy and computational cost.

ACKNOWLEDGEMENT

This work is supported by the National Natural Science Foundation of China, "Study on Aerodynamic Optimization Theroy and Method for Cascades of Turbomachinery beased on Control Theory", Project No.50776065.

Appendix A

In viscous flows, there are $\frac{\partial u_n}{\partial n}=0$ on the wall boundaries, therefore

$$\frac{\partial u_n}{\partial n}=\frac{\partial (u_i n_i)}{\partial x_j}n_j=n_i n_j\frac{\partial u_i}{\partial x_j}=0 \tag{51}$$

i.e. $n_i n_j\frac{\partial u_i}{\partial x_j}=0$ and $n_i n_j\frac{\partial u_j}{\partial x_i}=0$ (52)

The continuity equation in compressible flows takes the form as

$$\frac{\partial\left(\rho u_i\right)}{\partial x_i}=0 \tag{53}$$

i.e. $\rho\frac{\partial u_i}{\partial x_i}+u_i\frac{\partial \rho}{\partial x_i}=0$

due to the non-slip boundary condition of the N-S equations, there is $u_i=0$ on the wall, and there is $\rho>0$ in compressible flows. Hence,

$$\frac{\partial u_i}{\partial x_i}=0 \tag{54}$$

The viscous stresses are defined as

$$\tau_{ij}=\mu\left(\frac{\partial u_i}{\partial x_j}+\frac{\partial u_j}{\partial x_i}\right)+\lambda\delta_{ij}\frac{\partial u_k}{\partial x_k} \tag{55}$$

where, δ_{ij} is the Kronecker symbols.

With definition of the normal viscous stress $\sigma_n=n_i\tau_{in}=n_i n_j\tau_{ij}$. Hence,

$$\sigma_n=n_i n_j\left[\mu\left(\frac{\partial u_i}{\partial x_j}+\frac{\partial u_j}{\partial x_i}\right)+\lambda\delta_{ij}\frac{\partial u_k}{\partial x_k}\right] \tag{56}$$

Upon substitution of Eq.(52), Eq.(54) and $n_i n_i=1$ into Eq.(56), we can get

$$\sigma_n=0 \tag{57}$$

REFERENCES

[1] Newman, J. C., Taylor, A. C., Barnwell, R., Newman, P., and Hou, G. W., 1999, “Overview of Sensitivity Analysis and Shape Optimization for Complex Aerodynamic Configurations,” Journal of Aircraft, 36(2), pp.87-96.

[2] Pironneau, O., 1973, “On Optimum Shapes in Stokes Flow,” Journal of Fluid Mechanics, 59(2), pp.117-128.

[3] Jameson, A., 1988, “Aerodynamic Design via Control Theory,” Technical Report 88-64, ICASE.

[4] Reuther, J., and Jameson, A., 1994, “Control Based Airfoil Design Using the Euler Equations,” AIAA-94-4272-CP.

[5] Reuther, J., and Jameson, A., 1994, “Control Theory Based Airfoil Design for Potential Flow and a Finite Volume Discretization,” AIAA-94-0499.

[6] Jameson, A., Pierce, N. A., and Martinelli, L., 1997, “Optimum Aerodynamic Design Using the Navier-Stokes Equations,” AIAA 35th Aerospace Sciences Meeting & Exhibit, Reno, NV.

[7] Reuther, J., Jameson, A., Farmer, J., Martinelli, L., and Saunders, D., 1996, “Aerodynamic Shape Optimization of Complex Aircraft Configurations via an Adjoint Formulation,” AIAA-96-0094.

[8] Soto, O., and Loehner, R., 2000, “CFD Optimization Using an Incomplete-gradient Adjoint Approach,” AIAA-00-0666.

[9] Nadarajah, S., Jameson, A., and Alonso, J. J., 2002, “Sonic Boom Reduction Using an Adjoint Method for Wing-body Configurations in Supersonic Flow,” AIAA-02-5547.

[10] Yang, S., Wu, H., and Liu F., 2003, “Aerodynamic Design of Cascades by Using an Adjoint Equation Method,” AIAA-2003-1068.

[11] Arens, K., Rentrop, P., Stoll, S. O., and Wever, U., 2005, “An Adjoint Approach to Optimal Design of Turbine Blades,” Applied Numerical Mathematics, 53, pp,93-105.

[12] Campobasso, M. S., Duta, M., and Giles M. B., 2001, “Adjoint Methods for Turbomachinery Design,” ISABE Paper, ISABE-2001-1055.

[13] Florea, R., and Hall, K. C., 2001, “Sensitivity Analysis of Unsteady Inviscid Flow through Turbomachinery Cascades,” AIAA Journal, 39(6), pp.1047-1056.

[14] Wu, H., Liu, F., and Tsai, H., 2005, “Aerodynamic Design of Turbine Blades Using an Adjoint Equation Method,” AIAA-05-1006.

[15] Papadimitriou, D. I., and Giannakoglou, K. C., 2006, “Compressor Blade Optimization Using a Continuous Adjoint Formulation,” ASME Paper GT2006-90466.

[16] Papadimitriou, D. I., and Giannakoglou, K. C., 2007, “A Continuous Adjoint Method with Objective Function Derivatives Based on Boundary Integrals for Inviscid and Viscous Flows,” Computers & Fluids, 36, pp.325-341.

[17] Li, Y. C., Yang, D. L., and Feng, Z. P., 2006, “Inverse Problem in Aerodynamic Shape Design of Turbomachinery Blades,” ASME Paper GT2006-91135.

[18] Li, Y. C., and Feng, Z. P., 2007, “Aerodynamic Design of Turbine Blades by Using Adjoint-Based Method and N-S Equation,” ASME Paper GT2007-27734.

[19] Li, Y. C., and Feng, Z. P., 2008, “Three-Dimensional Aerodynamic Design of Turbine Blades Using the Adjoint Method,” ASME Paper GT2008-51225.

[20] Wang, D. X., and He, L., 2008, “Adjoint Aerodynamic Design Optimization for Blades in Multi-Stage Turbomachines: Part I -Methodology and Verification,” ASME Paper GT2008-50208.

[21] Wang, D. X., He, L., Li, Y. S., Wells, R. G., and Chen, T., 2008, “Adjoint Aerodynamic Design Optimization for Blades in Multi-Stage Turbomachines: Part II -Validation and Application,” ASME Paper GT2008-50209.

[22] Li, H. T., Song, L. M., Li, Y. C., and Feng, Z. P., 2009, “2D Viscous Aerodynamic Shape Design Optimization for Turbine Blades Based on Adjoint Method,” ASME Paper GT 2009-59999, also to be published in ASME Journal of Turbomachinery, 2011, 133(2).

[23] Luo, J. Q., Xiong, J. T., Liu, F., and McBean, I., 2010, “Secondary Flow Reduction by Blade Redesign and Endwall Contouring Using an Adjoint Optimization Method,” ASME Paper GT2010-22061.

[24] Wang, D. X., and Li, Y. S., 2010, “3D Direct and Inverse Design Using NS Equations and the Adjoint Method for Turbine Blades,” ASME Paper GT2010-22049.

[25] Marta, A. C., Van der Weide, E., Alonso, J. J., Mader, C. A., and Martins, J. R. R. A., 2007, “Adjoint: A methodology for the development of discrete adjoint solvers using automatic differentiation tools,” International Journal of Computational Fluid Dynamics, 21(9-10), pp.307-327.

[26] Blazek, J., 2001, “Computational Fluid Dynamics: Principles and Applications,” Elsevier, 1st Edition.